Path Planning for Flexible Needles Using Second Order Error Propagation

Wooram Park, Yunfeng Wang, and Gregory S. Chirikjian

Abstract. In this paper we propose a computationally efficient method for the steering of flexible needles with a bevel tip in the presence of uncertainties for the case when there are no obstacles in the environment. Based on the stochastic model for the needles, we develop a new framework for path planning of a flexible needle with a bevel tip. This consists of three parts: (a) approximation of probability density functions for the needle tip pose; (b) application of a second order error propagation algorithm on the Euclidean motion group; and (c) application of the path-of-probability (POP) algorithm. The probability density functions are approximated as Gaussians under the assumption that the uncertainty in the needle insertion is fairly small. The means and the covariances for the probability density functions are estimated using the error propagation algorithm that has second order accuracy. The POP algorithm is adapted to the path planning for the flexible needles so as to give the appropriate steering plan. Combining these components and considering 5 degree-of-freedom targets, the new method gives the path of the flexible needle that hits the target point with the desired hitting direction.

1 Introduction

A number of recent works have been reported on the topic of the steerable flexible needles with bevel tips that are inserted into soft tissue for minimally invasive

Wooram Park and Gregory S. Chirikjian
Department of Mechanical Engineering, Johns Hopkins University,
Baltimore, MD 21218, USA
e-mail: {wpark7,gregc}@jhu.edu

Yunfeng Wang
Department of Mechanical Engineering, The College of New Jersey, Ewing,
NJ 08628 USA
e-mail: jwang@tcnj.edu

G.S. Chirikjian et al. (Eds.): Algorithmic Foundations of Robotics VIII, STAR 57, pp. 583–595.
springerlink.com

medical treatments [1, 2, 7, 12, 17]. In this problem, a flexible needle is rotated with the angular speed $\omega(t)$ around its tangent while it is inserted with translational speed $v(t)$ in the tangential direction. Due to the bevel tip, the needle will not follow a straight line even when $\omega(t) = 0$ and $v(t)$ is constant. Rather, in this case the tip of the needle will approximately follow a circular arc with curvature κ when the medium is very firm and the needle is very flexible. The specific value of the constant κ depends on parameters such as the angle of the bevel, how sharp the needle is, and properties of the tissue. In practice κ is fit to experimental observations of the needle bending in a particular medium during insertions with $\omega(t) = 0$ and constant $v(t)$. Using this as a baseline, and building in arbitrary $\omega(t)$ and $v(t)$, a nonholonomic kinematic model then predicts the time evolution of the position and orientation of the needle tip [12, 17].

One of the most important tasks related to this flexible needle is that we should control the needles in order to get the desired tip position with or without the desired final direction, because the needles are used for drug injection or biopsy at a specific location. The path obtained by planning algorithms will be used for the actual control of the needle. In this paper, we focus on the path planning for the flexible needle.

A stochastic model for the steering of flexible needles with bevel tips has been developed in [12, 13]. It adopted the unicycle nonholonomic kinematic model [17]. Furthermore, it includes white noises weighted by coloring constants to capture the nondeterministic behavior of the needle insertion. This method, which is reviewed in detail in Section 2.2, is modified in this paper in such a way that allows for the closed-form evaluation of probability densities. The benefit of the closed-form method developed here is that it enables fast path planning. In order to evaluate the parameters that serve as the input to this closed-form probability density, the kinematic covariance propagation method developed in [14] is used. This probability density function is used for the path planning that was developed in [12, 13]. Like the work by Mason and Burdick [11], this path planning algorithm is an extension of the path-of-probability (POP) algorithm presented in [8]. Duindam et al. presented a path planning method for 3D flexible needle steering [7]. Although they consider 3D needle steering with obstacles, only positions of the targets are aimed for in that work. Our method gives a path that hits the goal position with the "desired direction" in a 3D environment without obstacles.

There exist some methods for steering nonholonomic systems [10]. Since some of them use the concept of optimal control, it is computationally intensive. Furthermore, since the needle system is not small-time locally controllable [12], the small changes in the goal pose can lead to large changes in the optimal path. We also note that Brockett's theorem says that some nonholonomic systems can not be stabilized to a desired pose using a continuous feedback. The POP algorithm used for the needle path planning in this paper has benefits compared to the existing methods based on optimal path following or optimal control: (1) At each time step we can make a choice about what control input to use, independent of the previous step, which means that this control is discontinuous and the limitations imposed by Brockett's theorem do not apply; (2) The path that we generate is not the path of minimal

length, or optimal, and so the solution is not as sensitive to small changes in the desired position as methods based on optimal control. Of course, this means that our paths may be a little bit longer, but we believe that they are also more robust to perturbations.

2 Mathematical Methods

2.1 Review of Rigid-Body Motions

The special orthogonal group, SO(3), is the space of rotation matrices contained in $\mathbb{R}^{3\times 3}$, together with the operator of matrix multiplication. Any element of SO(3) can be written using the Euler angles as [6]

$$R = R_z(\alpha)R_x(\beta)R_z(\gamma),$$

where α, β and γ are the ZXZ Euler angles, $0 \le \alpha, \gamma \le 2\pi$, $0 \le \beta \le \pi$ and

$$R_z(\theta) = \begin{pmatrix} \cos\theta & -\sin\theta & 0 \\ \sin\theta & \cos\theta & 0 \\ 0 & 0 & 1 \end{pmatrix}, \qquad R_x(\theta) = \begin{pmatrix} 1 & 0 & 0 \\ 0 & \cos\theta & -\sin\theta \\ 0 & \sin\theta & \cos\theta \end{pmatrix}.$$

The Euclidean motion group, SE(3), represents rigid-body motions in 3D space. It is the semi-direct product of $\mathbb{R}^3$ with SO(3). The elements of SE(3) can be written as [6]

$$g = \begin{pmatrix} R & \mathbf{t} \\ \mathbf{0}^T & 1 \end{pmatrix}, \tag{1}$$

where $R \in \mathrm{SO}(3)$, $\mathbf{t} \in \mathbb{R}^3$ and $\mathbf{0}^T$ denotes the transpose of the 3D zero vector.

Given a time-dependent rigid-body motion $g(t)$, the quantity

$$g^{-1}\dot{g} = \begin{pmatrix} R^T\dot{R} & R^T\dot{\mathbf{t}} \\ \mathbf{0}^T & 0 \end{pmatrix} \in se(3) \tag{2}$$

(where a dot represents the time derivative) is a spatial velocity as seen in the body-fixed frame, where $se(3)$ is the Lie algebra associated with SE(3). We identify $se(3)$ with $\mathbb{R}^6$ in the usual way via the mappings $^\vee : se(3) \to \mathbb{R}^6$ and $\widehat{\ } : \mathbb{R}^6 \to se(3)$, given by

$$\xi = (g^{-1}\dot{g})^\vee = \begin{pmatrix} (R^T\dot{R})^\vee \\ R^T\dot{\mathbf{t}} \end{pmatrix} = \begin{pmatrix} \omega \\ \mathbf{v} \end{pmatrix} \in \mathbb{R}^6$$

and

$$\widehat{\xi} = \widehat{\begin{pmatrix} \omega \\ \mathbf{v} \end{pmatrix}} = \begin{pmatrix} \widehat{\omega} & \mathbf{v} \\ \mathbf{0}^T & 0 \end{pmatrix} \in se(3),$$

where

$$\widehat{\omega} = \widehat{\begin{pmatrix} \omega_1 \\ \omega_2 \\ \omega_3 \end{pmatrix}} = \begin{pmatrix} 0 & -\omega_3 & \omega_2 \\ \omega_3 & 0 & -\omega_1 \\ -\omega_2 & \omega_1 & 0 \end{pmatrix}.$$

The vector ξ contains both the angular and translational velocity of the motion $g(t)$ as seen in the body-fixed frame of reference.

Let $\mathbf{e}_i$, $i = 1,\ldots,6$ denote the standard basis for $\mathbb{R}^6$. The basis given by a set of matrices $E_i = \widehat{\mathbf{e}}_i$, $i = 1,\ldots,6$ produce elements of SE(3), when linearly combined and exponentiated. Specifically we have [6]

$$E_1 = \begin{pmatrix} 0&0&0&0 \\ 0&0&-1&0 \\ 0&1&0&0 \\ 0&0&0&0 \end{pmatrix}; \quad E_2 = \begin{pmatrix} 0&0&1&0 \\ 0&0&0&0 \\ -1&0&0&0 \\ 0&0&0&0 \end{pmatrix}; \quad E_3 = \begin{pmatrix} 0&-1&0&0 \\ 1&0&0&0 \\ 0&0&0&0 \\ 0&0&0&0 \end{pmatrix};$$

$$E_4 = \begin{pmatrix} 0&0&0&1 \\ 0&0&0&0 \\ 0&0&0&0 \\ 0&0&0&0 \end{pmatrix}; \quad E_5 = \begin{pmatrix} 0&0&0&0 \\ 0&0&0&1 \\ 0&0&0&0 \\ 0&0&0&0 \end{pmatrix}; \quad E_6 = \begin{pmatrix} 0&0&0&0 \\ 0&0&0&0 \\ 0&0&0&1 \\ 0&0&0&0 \end{pmatrix}.$$

The element of SE(3) can be obtained by the exponential mapping as [6, 13]

$$g = g(x_1,x_2,...,x_6) = \exp\left(\sum_{i=1}^{6} x_i E_i\right).$$

Therefore the vector $\mathbf{x} = (x_1\ x_2\ \ldots\ x_6)^T$ can be obtained from $g \in \mathrm{SE}(3)$ by

$$\mathbf{x} = (\log g)^{\vee}.$$

If $X \in se(3)$ is an arbitrary element of the form

$$X = \begin{pmatrix} \Omega & \mathbf{v} \\ \mathbf{0}^T & 0 \end{pmatrix}, \quad \text{and} \quad \mathbf{x} = (X)^{\vee} = \begin{pmatrix} \omega \\ \mathbf{v} \end{pmatrix},$$

then $Ad(g)$ (the adjoint) is defined by the expression

$$(gXg^{-1})^{\vee} = Ad(g)\mathbf{x}, \ \text{ where } \ Ad(g) = \begin{pmatrix} R & 0 \\ TR & R \end{pmatrix}. \tag{3}$$

The matrix T is skew-symmetric, and $T^{\vee} = \mathbf{t}$, when $g \in \mathrm{SE}(3)$ is given as in (1).

2.2 Nonholonomic Stochastic Needle Model

In a reference frame attached to the needle tip with the local z axis denoting the tangent to the "backbone curve" of the needle, and x denoting the axis orthogonal to the direction of infinitesimal motion induced by the bevel (i.e., the needle bends in

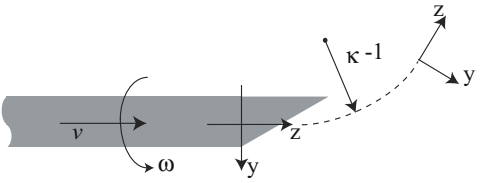

Fig. 1. The definition of parameters and frames in the nonholonomic needle model [12, 17].

the $y-z$ plane), the nonholonomic kinematic model for the evolution of the frame at the needle tip was developed in [12, 17] as:

$$\xi = (g^{-1}\dot{g})^{\vee} = \begin{bmatrix} \kappa \; 0 \; \omega(t) \; 0 \; 0 \; v(t) \end{bmatrix}^T, \tag{4}$$

where $\omega(t)$ and $v(t)$ are the rotation and insertion speeds, respectively. The frames and parameters for the needle are shown in Fig. 1.

If everything were certain, and if this model were exact, then $g(t)$ could be obtained by simply integrating the ordinary differential equation in (4). However, in practice a needle that is repeatedly inserted into a medium such as gelatin (which is used to simulate soft tissue [17]) will demonstrate an ensemble of slightly different trajectories.

A simple stochastic model for the needle is obtained by letting [12, 13]:

$$\omega(t) = \omega_0(t) + \lambda_1 w_1(t), \text{ and } v(t) = v_0(t) + \lambda_2 w_2(t).$$

Here $\omega_0(t)$ and $v_0(t)$ are what the inputs would be in the ideal case, $w_1(t)$ and $w_2(t)$ are uncorrelated unit Gaussian white noises, and λ_i are constants.

Thus, a nonholonomic needle model with noise is

$$(g^{-1}\dot{g})^{\vee}dt = \begin{bmatrix} \kappa \; 0 \; \omega_0(t) \; 0 \; 0 \; v_0(t) \end{bmatrix}^T dt + \begin{bmatrix} 0 & 0 & \lambda_1 & 0 & 0 & 0 \\ 0 & 0 & 0 & 0 & 0 & \lambda_2 \end{bmatrix}^T \begin{bmatrix} dW_1 \\ dW_2 \end{bmatrix} \tag{5}$$

where $dW_i = W_i(t+dt) - W_i(t) = w_i(t)dt$ are the non-differentiable increments of a Wiener process $W_i(t)$. This noise model is a stochastic differential equation (SDE) on SE(3). As shorthand, we write this as

$$(g^{-1}\dot{g})^{\vee}dt = \mathbf{h}(t)dt + Hd\mathbf{W}(t). \tag{6}$$

Corresponding to this SDE is the Fokker-Planck equation that describes the evolution of the probability density function of the ensemble of tip positions and orientations at each value of time, t [12, 13]:

$$\frac{\partial \rho(g;t)}{\partial t} = -\sum_{i=1}^{d} h_i(t)\tilde{E}_i^r \rho(g;t) + \frac{1}{2}\sum_{i,j=1}^{d} D_{ij}\tilde{E}_i^r \tilde{E}_j^r \rho(g;t) \tag{7}$$

where $D_{ij} = \sum_{k=1}^{m} H_{ik} H_{kj}^T$ and $\rho(g;0) = \delta(g)$. In (7) the "right" Lie derivative $\tilde{E}_i^r$ is defined for any differentiable function $f(g)$ as

$$\tilde{E}_i^r f(g) = \left(\frac{d}{dt} f(g \circ \exp(tE_i)) \right) \Big|_{t=0}. \tag{8}$$

For a small amount of diffusion, the solution for the Fokker-Planck equation, (7), can be approximated by a shifted Gaussian function [13, 15]:

$$\rho(g(\mathbf{x});t) = (2\pi)^{-3} |\det(\Sigma)|^{-1/2} \exp\left(-\frac{1}{2} (\mathbf{x} - \mu(t))^T \Sigma^{-1} (\mathbf{x} - \mu(t)) \right), \tag{9}$$

where $g = \exp(\hat{\mathbf{x}})$, and μ and Σ are the mean and the covariance of the probability density function, $\rho(g;t)$, respectively. This approximation is based on the fact that for small diffusion the Lie derivative is approximated as [13]

$$\tilde{E}_i^r f(g) \approx \frac{\partial f}{\partial x_i}.$$

Using this, the Fokker-Planck equation (7) becomes a diffusion equation in $\mathbb{R}^6$. Therefore, we have the solution for the diffusion equation as (9).

2.3 Second Order Error Propagation

If a unique value $\mu \in \mathrm{SE}(3)$ exists for which

$$\int_{\mathrm{SE}(3)} [\log(\mu^{-1}(t) \circ g)]^{\vee} \rho(g;t) dg = \mathbf{0},$$

then $\mu(t)$ is called the mean of a pdf $\rho(g,t)$. In addition, the covariance about the mean is defined as [16]

$$\Sigma(t) = \int_{\mathrm{SE}(3)} \log(\mu^{-1}(t) \circ g)^{\vee} [\log(\mu^{-1}(t) \circ g)^{\vee}]^T \rho(g;t) dg.$$

Suppose that for small values of t, the quantities $\mu(t)$ and $\Sigma(t)$ corresponding to $\rho(g;t)$ can be obtained (even if $\rho(g;t)$ is not known in closed form). Then these can be propagated over longer times. In other words, due to the Markovian nature of the above model, solutions can be "pasted together" using the fact that the following convolution equalities hold:

$$\rho(g;t_1 + t_2) = \rho(g;t_1) * \rho(g;t_2),$$

where convolution on $SE(3)$ is defined as in [5]. Even if these convolutions are too time-consuming to compute explicitly, the fact that these expressions hold means that propagation formulas for the mean and covariance can be used.

Wang and Chirikjian [16] derived the formulas for the second order propagation. If a pdf, $\rho_i(g)$ has mean μ_i and covariance Σ_i for $i = 1,2$, then with second order accuracy, the mean and covariance of $(\rho_1 * \rho_2)(g)$ are respectively [6]

$$\mu_{1*2} = \mu_1 \circ \mu_2 \qquad \text{and} \qquad \Sigma_{1*2} = A + B + F(A,B), \tag{10}$$

where $A = Ad(\mu_2^{-1})\Sigma_1 Ad^T(\mu_2^{-1})$, $B = \Sigma_2$ and $F(A,B)$ is given in Appendix. Consequently, we can obtain the mean and covariance for a relatively large t with given mean and covariance for a small t by this propagation formulas. These can then be substituted into (9) to obtain a closed-form estimate of the probability density that the needle will reach any particular pose at any value of time.

3 Path Planning for Flexible Needles

For path planning, we use the algorithm that appeared in [12, 13]. This algorithm was adapted from the path-of-probability algorithm in [8]. A similar trajectory planning method can be also found in [11].

In this algorithm, we find the whole path by serially pasting together several intermediate paths. Fig. 2. shows the concept of this algorithm. We aim to find a path that starts at g_0 and ends at g_{goal} using M intermediate steps. The homogeneous transformation matrix, $g_i \in \mathrm{SE}(3)$ $(i = 1,2,...,M)$, represents the position and orientation of the ith frame with respect to $(i-1)$th frame as shown in Fig. 2. Suppose that the $(i-1)$ intermediate steps $(g_1, g_2, \cdots, g_{i-1} \in \mathrm{SE}(3))$ have been already determined. The intermediate step, g_i is determined to maximize the probability that the remaining steps reach the goal. In Fig. 2, the shaded ellipses depict the probability density function when we consider the remaining $(M-i)$ steps. In other words, when we consider $(M-i)$ intermediate steps after g_i, the final pose will be in the dark area with higher probability than the bright area. Comparing the two simplified cases in Fig. 2, if the previous intermediate steps $(g_1, g_2, \cdots, g_{i-1})$ are the same for both cases, we should choose g_i as shown in Fig. 2b, because it guarantees the higher probability that the final pose reaches the goal pose.

The determination of the intermediate steps can be formulated as

$$g_i = \arg\max_{g \in S} \rho\left((g_0 \circ g_1 \cdots g_{i-1} \circ g)^{-1} \circ g_{goal}; \tau_i\right), \tag{11}$$

where τ_i is the remaining time to hit the goal and S is the set of possible intermediate poses. Now let us adapt this to the needle insertion problem. If t_{total} is the fixed time for the insertion from g_0 to g_{goal} and we have M intermediate steps, each intermediate step takes $\Delta t = t_{total}/M$. Therefore, we can define $\tau_i = (M-i)t_{total}/M$ in (11). Technically, this formula can not be used for determining the final intermediate step, g_M, because there is no remaining path. The final step can be determined to minimize the difference between the resulting final pose of the path and the goal pose using metrics such as in [4, 9].

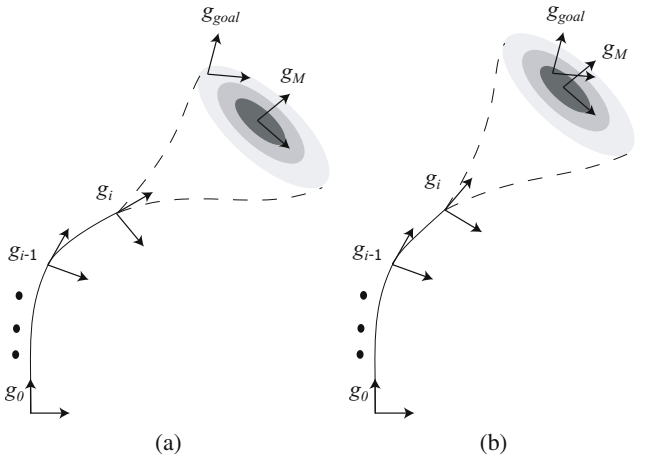

Fig. 2. The path-of-probability algorithm at the ith step. (a) Evaluation of one candidate move, g_i, with low resulting probability of reaching goal, (b) an intermediate step, g_i, resulting in high probability of reaching the goal.

Since the flexible needle that we consider is usually controlled by rotating along the axis tangential to the needle curve under the constant insertion speed, the above algorithm can be modified into the following: The intermediate step, g_i can be determined by

$$\theta_i = \underset{\theta\in[0\,2\pi)}{\arg\max}\,\rho((g_0 \circ g_1 \cdots g_{i-1} \circ \tilde{R}(\theta) \circ \mu(\Delta t))^{-1} \circ g_{goal}; (M-i)t_{total}/M), \quad (12)$$

$$g_i = \tilde{R}(\theta_i) \circ g_{\Delta t} \quad (13)$$

where

$$\tilde{R}(\theta) = \begin{pmatrix} R_z(\theta) & \mathbf{0} \\ \mathbf{0}^T & 1 \end{pmatrix}$$

and $g_{\Delta t}$ is one sample path obtained by integrating the SDE (6) up to time $t = \Delta t = t_{total}/M$ (which is our model for what a real needle would do over this period of time), and $\mu(\Delta t)$ is the sample mean of the SDE (6) at the time $t = \Delta t = t_{total}/M$. The resulting whole path is given as $g = g_0 \circ g_1 \cdots g_M$. This insertion is achieved by repeating the twisting without insertion and the insertion without twisting.

It is important to understand why $\mu(\Delta t)$ and $g_{\Delta t}$ are used in (12) and (13), respectively. When determining θ_i using (12), the ith insertion has not been actually performed. In order to evaluate the probability, we need an estimate for the simple insertion after the rotation. Since our needle insertion system has the stochastic behavior, the mean path, $\mu(\Delta t)$, is the reasonable choice for the estimate. After obtaining θ_i, we need to define g_i carefully. The ith intermediate step, g_i, is that we twist the needle by θ_i and then insert it with constant insertion speed without twisting. Since the simple insertion is the "actual" insertion, this should not be the

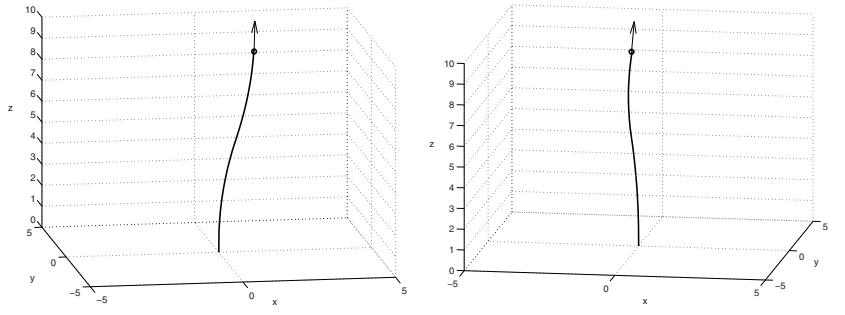

(a) (b)

Fig. 3. Results of path planning for the flexible needles. The thin arrow shows the desired direction of the needle and the circle shows the target position. (a) Needle path for the goal, $(\alpha, \beta, p_x, p_y, p_z) = (0, 0.1, 1, -1, 9.8)$ (b) Needle path for the goal, $(\alpha, \beta, p_x, p_y, p_z) = (\pi/4, 0.1, 0, -1.5, 9.8)$

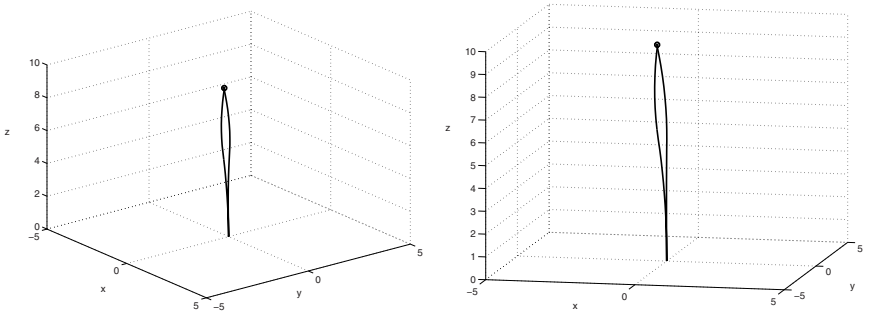

(a) (b)

Fig. 4. Results of path planning for the flexible needles. (a) Needle paths for the goals, $(\alpha, \beta, p_x, p_y, p_z) = (0, 0.1, 1, -1, 9.8)$ and $(\pi/2, 0.1, 1, -1, 9.8)$ (b) Needle paths for the goals, $(\alpha, \beta, p_x, p_y, p_z) = (\pi/4, 0.1, 0, -1.5, 9.8)$ and $(-\pi/4, 0.1, 0, -1.5, 9.8)$

mean path. Rather, one sample path obtained by integrating the SDE (6) up to time $t = \Delta t = t_{total}/M$ is more realistic choice as in (13).

In practice, $\mu(\Delta t)$ can be approximated by noise-free path that can be obtained by integrating the deterministic model (4) up to $t = \Delta t$, if $\|D\Delta t\|$ is small. D was defined in (7). In addition, the first covariance $\Sigma(\Delta t)$ that will be put in the propagation formula can be approximated by $D\Delta t$, because the diffusion by the noise term in SDE is small. Using the propagation formulas in (10) with the mean and covariance at $t = \Delta t$, we can compute the mean and covariance at $t = 2\Delta t, 3\Delta t, \cdots, M\Delta t$. Plugging these means and covariances into (9), we obtained the closed-form probability density function, $\rho(g;t)$. We use this pdf for the POP path planning algorithm.

In the real flexible needle system, if we twist the needle without insertion after the needle tip hits a target, the whole shape of the needle does not change. Therefore, out of 6 degrees of freedom of the target, we can naturally specify 5 degrees of freedom of the target pose using the desired position and direction. The remaining

rotational DOF (twisting around the needle backbone curve) can be considered as a free parameter which will be determined to guarantee the reacheability of the needle insertion system.

The target pose of the needle can be written as

$$g_{target} = \begin{pmatrix} R_z(\alpha)R_x(\beta)R_z(\gamma) & \mathbf{p} \\ \mathbf{0}^T & 1 \end{pmatrix},$$

where $\mathbf{p}$ is a 3D position vector. First we specify the 5 degrees of freedom: α, β and $\mathbf{p}$ using the desired position and direction of the needle tip. Then, for various values of γ, we repeatedly perform the path planning algorithm until we have a reasonable path.

Fig. 3 shows the paths obtained by the suggested method. We used the parameter values, $\kappa = 0.0449$, $\lambda_1 = 0.08$ and $\lambda_2 = 0.015$. We also set $\omega_0(t) = 0$ and $v_0(t) = 1$ in (5). We used 20 intermediate steps. Using a current PC (Intel Core Duo processor 2.66GHz, 1GB memory) the propagation (10) takes 0.33(sec) for 20 intermediate steps. For given α, β, γ and $\mathbf{p}$, the POP algorithm (12) and (13) gives a result in 0.37(sec), when we use 50 candidates for θ in (12), which are equally-spaced from 0 to 2π(rad). In the example in Fig. 3a, we tested with the 18 candidates for γ, equally-spaced from 0 to 2π(rad) and we could find the path with $\gamma = 4.89$(rad). Fig. 4 shows that for the same target position, we can have different paths applying different desired directions.

4 Conclusions and Discussions

In this work, we proposed a path planning method for the flexible needle. This method mainly uses the path-of-probability algorithm which requires the probability density function. Based on the stochastic model for the needle insertion, we approximated the probability density function for the needle tip pose with a shifted Gaussian distribution and obtained the mean and covariance for the probability density function using the second order error propagation theory. Using the path-of-probability algorithm, the needle paths that reach the goal position along the desired direction were obtained. Since the propagation formulas need the mean and covariance for the short length as inputs and compute the mean and covariance for the relatively long length as outputs, we only have to sample the needle path for the short length. Therefore we could avoid extensive sampling and long-range integration which are time-consuming.

This new method has two advanced features. First it uses the second order propagation formulas which is more accurate than the first order one that was used in [13]. Second, it can deal with the desired final direction of the needle tip, which was ignored in [7, 12, 13]. Using the second feature, we can generate a needle path avoiding an obstacle in an indirect way. Fig. 4 shows the possibility of obstacle avoidance.

We approximated the probability density function as a Gaussian assuming small diffusion. Thus evaluation of the probability density function is less reliable in a

distant area from the mean. This aspect eventually affects the performance of our path planning method. Specifically, if the desired position and orientation of the needle are away from the mean path, the path planning method does not always guarantee to give a reasonable path. One solution would be that we should start with a stochastic model which reflects the given target pose. In this paper, we considered only one case where the noise-free path is a simple circular arc.[1] If we consider another noise-free path that can be obtained by changing $\omega_0(t)$ and $v_0(t)$ in (5), the path planning method will work for more various target poses. Future research should include the method of determining $\omega_0(t)$ and $v_0(t)$ which reflect the given target pose for better performance of the path planning method.

Acknowledgements. This work was supported by NIH Grant R01EB006435 "Steering Flexible Needles in Soft Tissue."

Appendix

We review the second order propagation formulae. The entire work including derivation appears in [16].

If a pdf, $\rho_i(g)$, has mean μ_i and covariance Σ_i for $i = 1,2$, then to second order, the mean and covariance of $(\rho_1 * \rho_2)(g)$ are respectively [6]

$$\mu_{1*2} = \mu_1 \circ \mu_2 \text{ and } \Sigma_{1*2} = A + B + F(A,B),$$

where $A = Ad(\mu_2^{-1})\Sigma_1 Ad^T(\mu_2^{-1})$, $B = \Sigma_2$. Here

$$F(A,B) = C(A,B)/4 + (A''B + (A''B)^T + B''A + (B''A)^T)/12$$

A'' is computed as

$$A'' = \begin{pmatrix} A_{11} - \mathrm{tr}(A_{11})I_3 & 0_3 \\ A_{12} + A_{12}^T - 2\mathrm{tr}(A_{12})I_3 & A_{11} - \mathrm{tr}(A_{11})I_3 \end{pmatrix},$$

where A_{ij} are 3×3 block matrices in

$$A = \begin{pmatrix} A_{11}\ A_{12} \\ A_{12}^T\ A_{22} \end{pmatrix}.$$

B'' is defined in the same way with B replacing A everywhere in the expression. The blocks of C are computed as

$$C_{11} = -D_{11,11}$$

[1] Mathematically, the noise-free path and the mean path are not the same in the stochastic model for the flexible needle. However, we can treat them as the same in practice when the diffusion is small.

$$C_{12} = -(D_{21,11})^T - D_{11,12} = C_{21}$$
$$C_{22} = -D_{22,11} - D_{21,21} - (D_{21,12})^T - D_{11,22}$$

where $D_{ij,kl} = D(A_{ij}, B_{kl})$, and the matrix-valued function $D(A', B')$ is defined relative to the entries in the 3×3 blocks A' and B' as

$$d_{11} = -a'_{33}b'_{22} + a'_{31}b'_{32} + a'_{23}b'_{23} - a'_{22}b'_{33}, \qquad d_{12} = a'_{33}b'_{21} - a'_{32}b'_{31} - a'_{13}b'_{23} + a'_{21}b'_{33},$$
$$d_{13} = -a'_{23}b'_{21} + a'_{22}b'_{31} + a'_{13}b'_{22} - a'_{12}b'_{32}, \qquad d_{21} = a'_{33}b'_{12} - a'_{31}b'_{32} - a'_{21}b'_{13} + a'_{21}b'_{33},$$
$$d_{22} = -a'_{33}b'_{11} + a'_{31}b'_{31} + a'_{13}b'_{13} - a'_{11}b'_{33}, \qquad d_{23} = a'_{23}b'_{11} - a'_{21}b'_{31} - a'_{13}b'_{12} + a'_{11}b'_{32},$$
$$d_{31} = -a'_{32}b'_{12} + a'_{31}b'_{22} + a'_{22}b'_{13} - a'_{21}b'_{23}, \qquad d_{32} = a'_{32}b'_{11} - a'_{31}b'_{21} - a'_{12}b'_{13} + a'_{11}b'_{23},$$
$$d_{33} = -a'_{22}b'_{11} + a'_{21}b'_{21} + a'_{12}b'_{12} - a'_{11}b'_{22}.$$

References

1. Alterovitz, R., Goldberg, K., Okamura, A.: Planning for Steerable Bevel-tip Needle Insertion Through 2D Soft Tissue with Obstacles. In: IEEE Int. Conf. on Robot. and Auto., pp. 1652–1657 (2005)
2. Alterovitz, R., Siméon, T., Goldberg, K.: The Stochastic Motion Roadmap: A Sampling Framework for Planning with Markov Motion Uncertainty. In: Proc. Robot. Sci. and Syst. (2007)
3. Brockett, R.W.: Asymptotic stability and feedback stabilization. Differential Geometric Control Theory, 181–208 (1983)
4. Chirikjian, G.S., Zhou, S.: Metrics on Motion and Deformation of Solid Models. ASME J. Mech. Des. 120(2), 252–261 (1998)
5. Chirikjian, G.S., Ebert-Uphoff, I.: Numerical Convolution on the Euclidean Group with Applications to Workspace Generation. IEEE Trans. on Robot. and Auto. 14(1), 123–136 (1998)
6. Chirikjian, G.S., Kyatkin, A.B.: Engineering Applications of Noncommutative Harmonic Analysis. CRC Press, Boca Raton (2000)
7. Duindam, V., Alterovitz, R., Sastry, S., Goldberg, K.: Screw-Based Motion Planning for Bevel-Tip Flexible Needles in 3D Environments with Obstacles. In: IEEE Int. Conf. on Robot. and Auto., pp. 2483–2488 (2008)
8. Ebert-Uphoff, I., Chirikjian, G.S.: Inverse Kinematics of Discretely Actuated Hyper-Redundant Manipulators Using Workspace Densities. In: IEEE Int. Conf. on Robot. and Auto., pp. 139–145 (1996)
9. Kuffner, J.J.: Effective Sampling and Distance Metrics for 3D Rigid Body Path Planning. In: IEEE Int. Conf. on Robot. and Auto., pp. 3993–3998 (2004)
10. Laumond, J.P. (ed.): Robot Motion Planning and Control. LNCIS, vol. 229. Springer, New York (1998)
11. Mason, R., Burdick, J.W.: Trajectory Planning Using Reachable-State Density Functions. In: IEEE Int. Conf. on Robot. and Auto., pp. 273–280 (2002)
12. Park, W., Kim, J.S., Zhou, Y., Cowan, N.J., Okamura, A.M., Chirikjian, G.S.: Diffusion-based motion planning for a nonholonomic flexible needle model. In: IEEE Int. Conf. on Robot. and Auto., pp. 4600–4605 (2005)
13. Park, W., Liu, Y., Zhou, Y., Moses, M., Chirikjian, G.S.: Kinematic State Estimation and Motion Planning for Stochastic Nonholonomic Systems Using the Exponential Map. Robotica, 419–434 (2008)

14. Wang, Y., Chirikjian, G.S.: Second-Order Theory of Error Propagation on Motion Groups. WAFR, New York City (2006)
15. Wang, Y., Chirikjian, G.S.: Error Propagation on the Euclidean Group with Applications to Manipulator Kinematics. IEEE Trans. on Robot. 22(4), 591–602 (2006)
16. Wang, Y., Chirikjian, G.S.: Nonparametric Second-Order Theory of Error Propagation on Motion Groups. Int. J. of Robot. Res. 27, 1258–1273 (2008)
17. Webster III, R.J., Kim, J.S., Cowan, N.J., Chirikjian, G.S., Okamura, A.M.: Nonholonomic modeling of needle steering. Int. J. of Robot. Res. 25, 509–525 (2006)